Journal of Biomedical Optics

BiomedicalOptics.SPIEDigitalLibrary.org

Experimentally observe the effect of spherical aberration on diffractive intraocular lens using adaptive optics

Huanqing Guo
Elie DeLestrange

SPIE.

Experimentally observe the effect of spherical aberration on diffractive intraocular lens using adaptive optics

Huanqing Guo[a,b,*] and Elie DeLestrange[a]
[a]National University of Ireland Galway, School of Physics, Applied Optics Group, University Road, Galway, Ireland
[b]R&D, Detection and Vision System, Valeo, IDA Business Park, Dunmore Road, Tuam, Co. Galway, Ireland

Abstract. We first investigated the similarity in optical quality of a batch of diffractive intraocular lenses (DIOLs), providing experimental evidence for one DIOL as representative of a batch. Using adaptive optics, we then evaluated one DIOL under different levels of Zernike spherical aberration (SA) by applying both a point spread function test and a psychophysical visual acuity test. We found that for small aperture size SA has the effect of shifting the through-focus curve of DIOL. Also, for a relatively large aperture size, it has different effects on the distant and near foci. © *The Authors. Published by SPIE under a Creative Commons Attribution 3.0 Unported License. Distribution or reproduction of this work in whole or in part requires full attribution of the original publication, including its DOI.* [DOI: 10.1117/1.JBO.20.3.036008]

Keywords: diffractive lenses; adaptive optics; visual acuity; visual optics; metrology optics.

Paper 140855R received Dec. 23, 2014; accepted for publication Feb. 18, 2015; published online Mar. 12, 2015.

1 Introduction

With a passive mechanism for the treatment of presbyopia, diffractive intraocular lenses (DIOLs) are designed for the restoration of accommodation by creating multiple foci. The diffractive structure etched on the lens surface splits the light into different diffractive orders, forming two or more foci. Futhey[1] reported an early DIOL design which had +3.5 D added power in the 6-mm diameter area using 20 to 40 concentric zones with step height of a few microns. Since then, DIOLs have been studied by many authors in aspects of design, evaluation, and clinical implantation.[2–5] Clinically an implanted DIOL usually provides no improvement, or slightly worse visual quality for a distant object but significantly better quality for the near objects compared with a monofocal IOL.

Recent development of ocular wavefront aberration technology has suggested that IOLs should target more correction of aberration, especially spherical aberration (SA).[6] SA usually dominates over other ocular aberrations and statistically is not zero on average across the population.[7] The SA is distributed across the cornea and the crystalline lens for a normal eye, or the cornea and the IOL for a pseudophakic eye. The anterior corneal surface is the main contributor to the SA[8] and this may be corrected or increased with the following natural lens or artificial IOL. An SA compensating IOL has an aspheric such as a quadratic conic surface. Despite many variations in the pseudophakic eye's biometry and physiological parameters, the aspheric monofocal IOL still performs better than a spherical IOL.[9] For an aspheric DIOL, a theoretical simulation paper claimed that for large populations there is small percentage improvement if the DIOL has add-on of −0.1 μm SA (6 mm).[10]

For IOL evaluation, adaptive optics is a convenient facility to manipulate wavefront aberration. Equipped with a corrector such as a deformable mirror, an adaptive optics system is able to separate or combine different aberrations including an SA with a continuous amplitude.[11,12] Adaptive optics has been used to simulate the aberrations of an IOL,[13] test IOLs with produced aberrations,[14] and subjectively evaluate IOLs free from implantation.[15]

Given their sophisticated diffractive structure and foldable material, such as acrylic, whether a batch of DIOLs has similar optical quality remains a question. In this paper, we first examined and verified that a single DIOL's optical quality can represent a batch production of DIOLs. Based on this finding, we then investigated the effect of SA on a single DIOL with adaptive optics, applying both objective and subjective methods.

2 Experimental Methods

2.1 *Similarity Test of a Batch Product of DIOLs*

We measured the polychromatic point spread function (PSF) of a batch of DIOLs. The optical setup has been described elsewhere.[16] Briefly, a diffused white light point source from a polychromatic LED (Luxeon, 400 to 750 nm) passed through a model eye that consisted of an artificial corneal lens and a wet cell with a replaceable DIOL. A CCD camera captured the discrete PSF images from the point source. Altogether 12 bifocal DIOLs (Alcon, SN6AD3, apodized diffractive structure at central 3.6 mm, 20.0 D, added power +4.0 D at the IOL plane) were randomly divided into two groups of equal samples. The converging beam from the artificial cornea of the model eye provided a central circular aperture of 4.0 mm at the anterior surface of the DIOL. For each DIOL, PSF images at 12 locations were tested, including nine through-focus locations and three decentrations. The through-focus PSFs were recorded by translating the CCD backward/forward covering −0.4 to 0.4 mm with a 0.1 mm step, and the PSFs were also recorded at three decentrations by shifting the DIOL to right, left and down each by 0.5 mm. To avoid external off-axis aberrations, there was no objective lens used to magnify the PSF images.

*Address all correspondence to: Huanqing Guo, E-mail: huanqing.guo@nuigalway.ie.

As a contrast, one of these 12 DIOLs was repeatedly reloaded into the water cell and measured six times (each time at 12 locations as mentioned above), using the same procedure for testing each DIOL discussed above. The hypothesis is that the two data sets, one from the entire 12 DIOLs and the other from one DIOL, should have no significant difference. All the PSF images were processed as per the protocol described in Ref. 16. As a sensitive measurement of the distribution of the light intensity, the second-order moment of light distribution was calculated as the metric. The detailed results of this experiment are shown in Sec. 3; here, we refer to the conclusion of this experiment that one DIOL is representative of a batch of DIOLs. Therefore, we could apply only one DIOL in the next experiments.

2.2 *Effect of SA on DIOL—Bench Test of Point Spread Function*

This experiment is a through-focus PSF measurement for one DIOL with different values of SA. As shown in Fig. 1, the model eye consisting of a DIOL was combined with an adaptive optics system. The adaptive optics system incorporated two pairs of 4f lenses which provided three conjugating planes. The planes were those of the deformable mirror, the Hartman–Shack wavefront sensor, and the DIOL. The sensor calibrated and the deformable mirror generated the required SA while removing all other remaining aberrations. The deformable mirror, wavefront sensor, and their associated software (Imagine Eyes, France) together with the aberration control were similar to a previous study.[17] For defocus adjustment, a Badal system manually translated backward/forward along the optical axis. The model eye was on the same translational stage with the Badal system and they were capable of moving together. A 20×, 0.4 NA objective lens, operating on-axis only, was used to magnify the PSF images on a CCD.

An open loop operation was applied to generate SA. For a Zernike SA (Z(4,0)), precompensation and postcalibration were

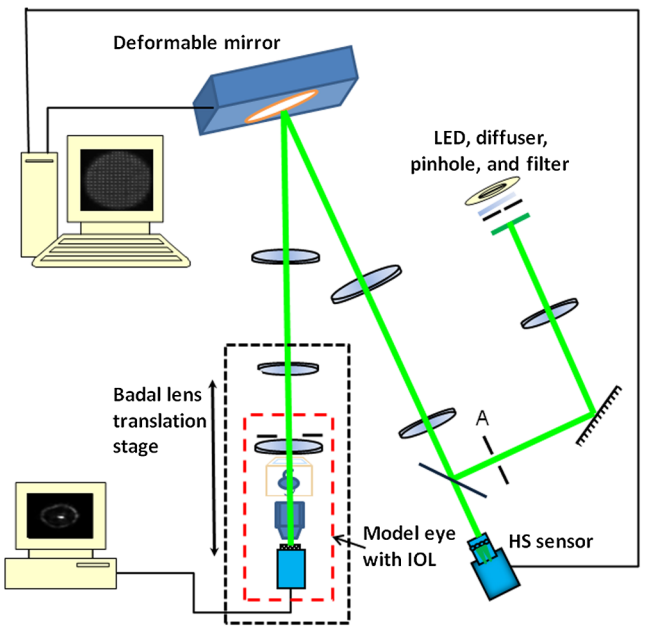

Fig. 1 Adaptive optics system and the model eye with a diffractive intraocular lens (DIOL) for point spread function (PSF) imaging.

necessary since it readily coupled with the defocus term.[12] Altogether nine levels of SA were used in this experiment. The coupled Zernike defocus calibrated by the wavefront sensor was considered together with the Badal system to yield a practical defocus value. The SA was induced in a system aperture (aperture A in Fig. 1 which conjugates with DIOL) whose size centrally covered 4.0-mm diameter on the DIOL. When the diameter was reduced to 2.5 mm, optical design software Zemax (Radiant Zemax Inc.) was used to calculate the Zernike SA and defocus coefficients, and the new coefficients for the smaller aperture were applied.

To determine the far and near foci of the DIOL and rescale the Badal lens, three rows of optotype letters were shown with a green organic LED microdisplay as the image target. The target was imaged on the CCD through the system. The two foci of the DIOL were determined at the position of the clearer images. Then a white LED (Luxeon) replaced the microdisplay. A rough surface diffuser followed by a 100-μm pinhole source provided a source point. A 550-nm central wavelength 10-nm bandwidth interference filter was used to provide monochromatic light. The CCD was a 12 bits (4096 gray level) monochromatic camera (Retiga 1300, Qimaging, peak response wavelength ~530 nm and FWHH ~400 nm) Its exposure time was optimized to have a maximum of 85% saturation at the best distant focus of the DIOL. For each PSF image, 10 sequential frames were acquired, digitalized, and averaged.

One of the DIOLs used in Sec. 2.1 was tested. We measured the through-focus PSF, covering −2.9 to +5.9 D (referring to the IOL added power) with approximately equal interval sampling of 15 to 17 points. This was done for each of the nine levels of SAs.

The processing of the PSF images, including computing the centroid, RMS radius, and second-order moment of light distribution has been described elsewhere.[16] Specifically for the through-focus DIOL, the compactness and contrast of the PSFs are of interest.[18] In order to filter the peripheral rings (see Fig. 3 for PSF examples) which are not critical to vision, we applied a two-dimensional Gaussian filter to all the PSF images centered at their centroids. The second-order moment of light distribution was calculated for each filtered PSF to be a measure of the compactness. The contrast was measured by the energy fraction in an encircled radius area. The encircled radius was selected as the smallest $D50$ radius (the radius where the enclosed PSF intensity fell at half of the whole PSF intensity) of all the PSF images. The metrics of compactness and contrast are inversely correlated. Taking the ratio of the compactness by the contrast, we formed a new metric:

$$\frac{\text{Compactness}}{\text{Contrast}} = \frac{\text{PSF second order light distribution}}{\text{PSF energy fraction in same area}}.$$

We call this the C/C metric that provides an empirical evaluation of the optical quality of the DIOL.

3 Results

For the first experiment of comparing a batching of DIOLs, we found that the two groups have no significant difference in their light distribution under any conditions. Figure 2 shows the results of 12 DIOLs compared to one DIOL reloading experiment. A paired t-test also shows statistically that the two data sets are equivalent ($p > 0.9$), which indicates that the batch product DIOLs have similar optical quality.

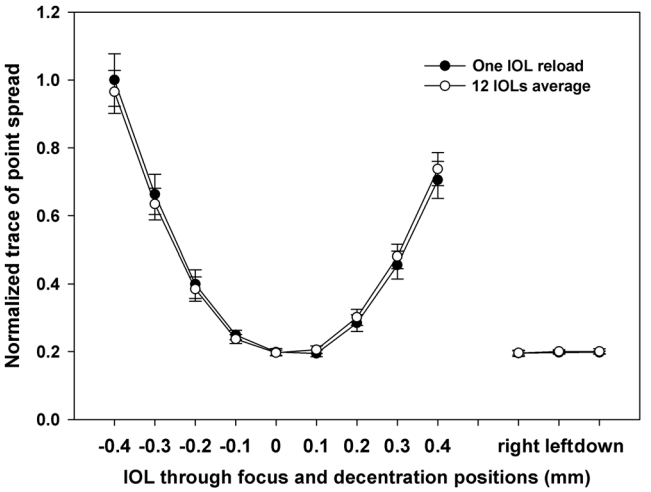

Fig. 2 DIOLs evaluated by PSFs through focus and with decentrations. The error bar shows ±1 standard deviation.

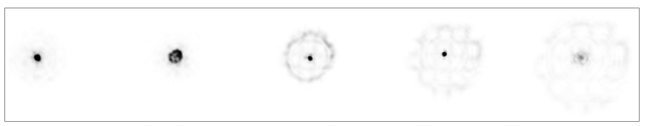

Fig. 3 Examples of the PSFs in a 4-mm diameter without spherical aberration (SA). The intensity scale is uniform (black indicates light distribution). Defocus amount from left to right, −0.5, 0.1, 2.3, 3.5, and 4.6 D.

For the PSF experiment, Fig. 3 presents some examples of the PSF images. The PSF central concentration and peripheral rings could be observed. Figure 4 shows the normalized C/C metric through the DIOL focus for different amounts of Zernike SA, at 4- and 2.5-mm diameters. In the left column in Fig. 4 for 4 mm, regardless of the sign of the SA, the curved peaks are extended at the distant foci and narrowed at the near foci. A positive SA shifted the curves to a more positive direction (hyperopic correction) and vice visa for a negative SA. The PSF compactness/contrast at the near foci is generally reduced due to SA. For the results of the 2.5 mm shown in the right column, a different SA only shifts both the distant and near foci.

4 Complementary Psychophysical Experiment

In order to further observe the subjective effect of SA on DIOL by the human eye, we performed a psychophysical experiment of through-focus visual acuity. With use of an unimplanted DIOL, this experiment was performed by an experienced subject using an adaptive optics system. A detailed description about the setup and the method has been published in Ref. 15. The DIOL was projected onto the subject's pupil with unit magnification. A four-alternatives forced choice psychophysical procedure with tumbling letter E was used to evaluate the visual acuity. The SA contribution of the subject's cornea and crystalline lens was measured, modeled, and separated through the simultaneous measurement of his anterior corneal topography and total eye wavefront aberration with an iDesign instrument (AMO). The subject's crystalline lens contributes −0.1 μm SA (4 mm) to compensate his corneal SA. To cancel the compensation, +0.1 μm

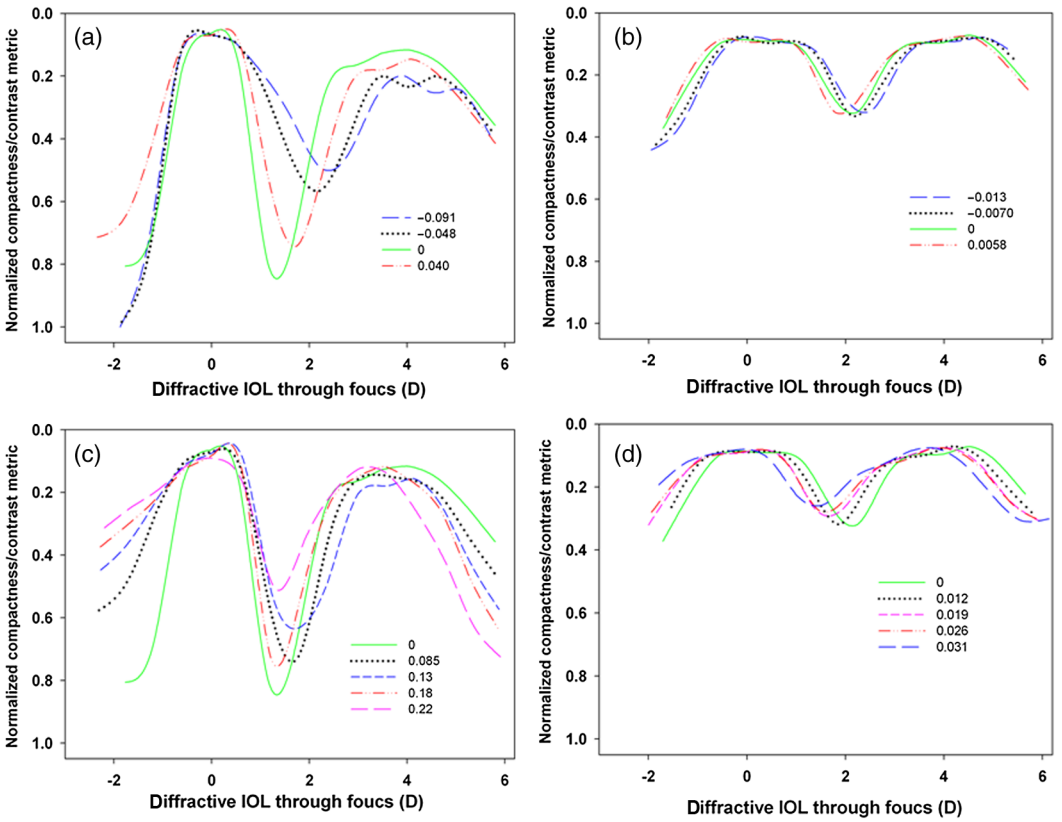

Fig. 4 C/C metric of the DIOL through-focus PSF. Different curves are for different levels of SA (unit: micron). Left and right columns are for 4- and 2.5-mm diameters, respectively; (a) and (b) for SA≤0; (c) and (d) for SA≥0.

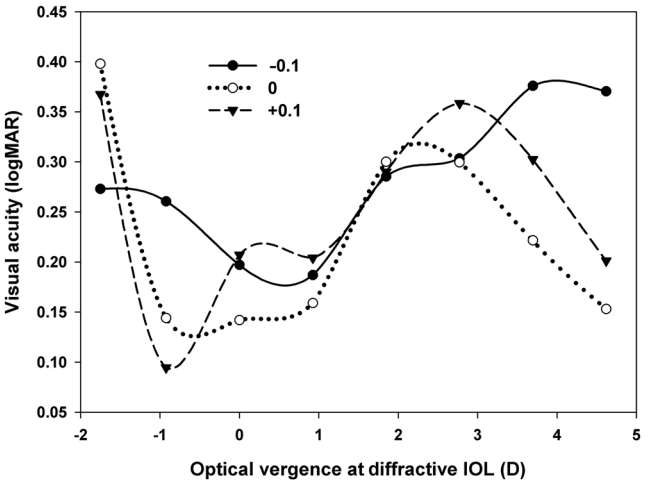

Fig. 5 Through-focus visual acuity at three levels of Zernike SA (unit: μm, 4 mm pupil). +0.1 μm SA cancels the subject's lens compensation, and 0 and −0.1 μm are shown as comparisons.

SA was induced by the adaptive optics. In contrast, another two levels of SA 0.0 and −0.1 μm were also used.

The research was approved by the Ethics Committee of National University of Ireland Galway. The subject's healthy right eye (0 D.S. −0.5 D.C. × 89) was instilled with one drop of 1% tropicamide 20 min before the experiment and another drop every hour during the experiment. The subject adjusted the Badal platform to search for his best distant focus through the DIOL, while looking at a 0.5 deg E letter shown on a green microdisplay (eMagin, 540-nm mean wavelength and FWHM 70-nm illumination). Based on the distant foci, the visual acuity at eight Badal positions was tested, each position with three levels of SA. These eight positions were approximately equal over the interval over covering the DIOL added power range of 0 to 4 D (0 to 3.1 D at the spectacle plane).

In one run of the visual acuity test, 120 E letters were randomly displayed in six steps of letter size in LogMAR, each for 0.3 s, and 50% was set as the correct answer threshold in a fitted plot of LogMAR letter size against correct answers. Two runs at each through-focus positions were performed, while if the outcome of these two runs had more than a 0.1 LogMAR difference, a third run would be performed. The average value was used as the estimation of the subject's visual acuity.

Figure 5 shows the results of the visual acuity experiment. First, the results confirmed the observation in Fig. 4 that positive SA shifts the through-focus curve to more hyperopic correction, in contrast to zero SA. The focus shifting is possibly due to the contribution of SA to the refraction power. Second, the results also suggest further separation between the two foci of the DIOL due to SA. The third point is that a positive SA could yield better visual acuity at distance foci of the DIOL. And the last point is that both positive and negative SAs would reduce the visual acuity at the near foci. We also noticed that a 0.1 μm SA in a 4 mm pupil is a relatively large value and there could be a limitation of the through focus range chosen in our study.

5 Discussions and Conclusion

The DIOL used in this study has an intensity apodization design.[2] The effective light energy diffracted to a focus varies as a function of the radial location on the lens. The SA is an optical phase addition which is independent of intensity apodization. A beam with SA bends to different directions from the center to the periphery. That is to say, the SA and the diffractive effects both cause the light redistribution. Hence, it is predictable that the two could interact with each other in complex way, dependent on the aperture sizes. For both apertures used in the bench test with SA, our analysis has avoided the absolute light intensity value, providing comparable evaluation of only the compactness and contrast. We are currently performing theoretical simulation of the DIOL, expecting more quantitative understandings of interaction between the SA and diffractive effect.

The +4 D DIOL has been designed to have −0.1 μm SA (6 mm).[10,19] This corresponds to about −0.02 μm at 4 mm. The physical model eye used in our bench test has about +0.02 μm intrinsic SA, just able to cancel the SA of the DIOL. This means the model eye with the DIOL inside it has no extra SA contribution.

The psychophysical visual acuity experiment was only performed by one subject with a normal eye free from DIOL implantation. In order to scale the DIOL's foci range, several subjects' eyes have performed observations through the DIOL and the adaptive optics system. The Badal optometer was calibrated to linearly scale the two foci of the DIOL. We found out that the added power of +4 D corresponded to +3.1 D at the spectacle plane. In Fig. 5, the calibration of the optical vergence was based on this finding.

Although the psychophysical visual acuity experiment included a band light source (FWHM ~ 70 nm), the chromatic effect throughout the visible spectrum has not been addressed in this study. Considering that the eye's SA should be independent on the visible wavelength especially in a small pupil size,[20] the chromatic SA is assumed to be small. However, longitudinal chromatic defocus, although possibly reducible by proper materials of the IOL,[21] can systematically degrade the image quality at both foci of a DIOL. As expected, SA may also interact with chromatic defocus and a theoretical study concluded that a small overall positive SA gives an optimized modulation transformation function for polychromatic light for DIOL.[22]

In summary, we carried out experiments to observe the SA effect on one DIOL after we verified that this single DIOL is representative. A mild positive SA can produce a better PSF quality than no SA.

Acknowledgments

We thank Professor Chris Dainty for his suggestions and comments. Financial support from Science Foundation Ireland (07/IN.1/1906), Enterprise Ireland (IR-2008-0014), and National Natural Science Foundation of China (No. 81170873).

References

1. J. A. Futhey, "Diffractive bifocal intraocular lens," *Proc. SPIE* **1052**, 142–149 (1989).
2. J. A. Davison and M. J. Simpson, "History and development of the apodized diffractive intraocular lens," *J. Cataract. Refract. Surg.* **32**, 849–858 (2006).
3. T. Eppig, K. Scholz, and A. Langenbucher, "Assessing the optical performance of multifocal (diffractive) intraocular lenses," *Ophthalmic Physiol. Opt.* **28**, 467–474 (2008).
4. J. F. Alfonso et al., "Visual quality after diffractive intraocular lens implantation in eyes with previous hyperopic laser *in situ* keratomileusis," *J. Cataract. Refract. Surg.* **37**, 1090–1096 (2011).

5. P. Artal et al., "Visual effect of the combined correction of spherical and longitudinal chromatic aberrations," *Opt. Express* **18**, 1637–1648 (2010).
6. J. T. Holladay et al., "A new intraocular lens design to reduce spherical aberration of pseudophakic eyes," *J. Refract. Surg.* **18**, 683–691 (2002).
7. L. N. Thibos et al., "Statistical variation of aberration structure and image quality in a normal population of healthy eyes," *J. Opt. Soc. Am. A* **19**, 2329–2348 (2002).
8. L. Wang et al., "Optical aberrations of the human anterior cornea," *J. Cataract. Refract. Surg.* **29**, 1514–1521 (2003).
9. H. Q. Guo, A. V. Goncharov, and C. Dainty, "Comparison of retinal image quality with spherical and customized aspheric intraocular lenses," *Biomed. Opt. Express* **3**, 681–691 (2012).
10. X. Hong and X. X. Zhang, "Optimizing distance image quality of an aspheric multifocal intraocular lens using a comprehensive statistical design approach," *Opt. Express* **16**, 20920–20934 (2008).
11. H. Q. Guo and D. A. Atchison, "Subjective blur limits for cylinder," *Optometry Vision Sci.* **87**, E549–E559 (2010).
12. D. A. Atchison and H. Q. Guo, "Subjective blur limits for higher order aberrations," *Optometry Vision Sci.* **87**, E890–E898 (2010).
13. C. Pérez-Vives et al., "Myopic astigmatism correction: comparison of a toric implantable collamer lens and a bioptics technique by an adaptive optics visual simulator," *Ophthalmic Physiol. Opt.* **33**, 114–122 (2013).
14. L. Zheleznyak et al., "Impact of corneal aberrations on through-focus image quality of presbyopia-correcting intraocular lenses using an adaptive optics bench system," *J. Cataract. Refract. Surg.* **38**, 1724–1733 (2012).
15. H. Guo et al., "Subjective evaluation of intraocular lenses by visual acuity measurement using adaptive optics," *Opt. Lett.* **37**, 1–3 (2012).
16. H. Guo, A. Goncharov, and C. Dainty, "Intraocular lens implantation position sensitivity as a function of refractive error," *Ophthalmic Physiol. Opt.* **32**, 117–124 (2012).
17. D. A. Atchison, H. Guo, and S. W. Fisher, "Limits of spherical blur determined with an adaptive optics mirror," *Ophthalmic Physiol. Opt.* **29**, 300–311 (2009).
18. L. N. Thibos et al., "Accuracy and precision of objective refraction from wavefront aberrations," *J. Vision* **4**, 329–351 (2004).
19. W. A. Maxwell, S. S. Lane, and F. Zhou, "Performance of presbyopia-correcting intraocular lenses in distance optical bench tests," *J. Cataract. Refract. Surg.* **35**, 166–171 (2009).
20. S. Marcos et al., "A new approach to the study of ocular chromatic aberrations," *Vision Res.* **39**, 4309–4323 (1999).
21. D. Siedlecki, M. Zajac, and J. Nowak, "Retinal images in a model of a pseudophakic eye with classic and hybrid intraocular lenses," *J. Mod. Opt.* **55**, 653–669 (2008).
22. X. Hong and M. Choi, "Influence of ocular longitudinal chromatic aberration on the selection of aspheric intraocular lenses," *Opt. Express* **18**, 26175–26183 (2010).

Huanqing Guo received his BSc, MEng, and PhD degrees in physics and optical engineering in China in 1999, 2002, and 2005, respectively. He had been a postdoctoral researcher at QUT of Australia from 2005 to 2009, researching optics and vision of the human eye with adaptive optics. In 2009, he joined the Applied Optics Group of NUI Galway in Ireland to investigate intraocular lenses. Since 2013, he has been an R&D engineer of the Detection and Vision System of Valeo Group.

Elie deLestrange received his master's degree in optics from the University of Paris VII in 2007, then joined the Applied Optics Group, NUI Galway, Ireland, where he received his PhD degree under the aegis of professor C. Dainty in May 2013. He is now a research scientist at the College of Biomedical Engineering, Peking University, China. His scientific interests are related to i1maging and visual psychophysics/cognition.